INVESTIGATION OF FAR-INFRARED SMITH-PURCELL RADIATION AT THE 3.41 MEV ELECTRON INJECTOR LINAC OF THE MAINZ MICROTRON MAMI

H. Backe, W. Lauth, H. Mannweiler, H. Rochholz,
K. Aulenbacher, R. Barday, H. Euteneuer, K.-H. Kaiser,
G. Kube, F. Schwellnus, V. Tioukine
Institut für Kernphysik, Universität Mainz, D-55099 Mainz, Germany
backe@kph.uni-mainz.de

Abstract An experiment has been set up at the injector LINAC of the Mainz Microtron MAMI to investigate far-infrared Smith-Purcell radiation in the THz gap (30 μm $\leq \lambda \leq$ 300μm). The essential components are a superconductive magnet with a magnetic induction of 5 Tesla in which 200 mm long gratings of various periods between 1.4 mm and 14 mm are located, and a composite silicon bolometer as radiation detector. First experiments were performed in the wavelength region between 100 μm and 1 mm with a bunched 1.44 MeV electron beam.

Keywords: Smith-Purcell radiation, FEL, SASE

Introduction

Smith-Purcell (SP) radiation is generated when a beam of charged particles passes close to the surface of a periodic structure, i.e., a diffraction grating. The radiation mechanism was predicted by Frank in 1942 [Frank, 1942] and observed in the visible for the first time by Smith and Purcell [Smith and Purcell, 1953] with an 250-300 keV electron beam. In a number of subsequent experiments the results were confirmed, for references see [Kube et al., 2002]. Soon after the discovery, potential applications of the SP effect became the topic of interest. In a number of theoretical and experimental studies the SP effect has been discussed as a basis for free electron lasers, for particle acceleration, or for particle beam diagnostics, for references see also [Kube et al., 2002]. In particular we mention the work of Urata et al. [Urata et al., 1998] in which superradiant Smith-Purcell Emission was observed for the first time at a wavelength λ = 491 μm with a 35 keV electron beam from a scanning electron microscope.

The optical radiation emission from diffraction gratings has been investigated at the Mainz Microtron MAMI using the low-emittance 855 MeV electron beam [Kube et al., 2002]. A general feature of SP radiation from optical diffraction gratings at ultrarelativistic beam energies is the weakness of the radiation. The reason was found in the smallness of the radiation factors $\mid R_n \mid^2$. According to Van den Berg's theory [Van den Berg, 1973a; Van den Berg, 1973b; Van den Berg, 1974; Van den Berg, 1971], these factors become only large at low electron beam energies.

In this contribution we report on first experiments with a 1.44 MeV beam at the injector of the Mainz Microtron MAMI to produce Smith-Purcell radiation in the wavelength region between 30-300 μm. Such radiation is of particular interest since in this so-called THz gap no compact and efficient radiation sources like lasers or electronic devices are currently available. In the following section, first some basic theoretical considerations underlying our experiments are described.

1. Basic Theoretical Background

According to the approach of di Francia [Di Francia, 1960] the radiation mechanism can be understood as the diffraction of the field of the electron by the grating. It is diffracted in radiating and non-radiating orders. The latter are evanescent surface waves with a phase velocity which might coincide with the velocity of the electron. In this case the electron can transfer energy to the wave and indirectly drive the radiating orders. The angular distribution of the number of photons dN per electron radiated into the nth order into the solid angle $d\Omega$ is

$$\frac{dN}{d\Omega} = \alpha \mid n \mid N_W \frac{\sin^2\Theta \sin^2\Phi}{(1/\beta - \cos\Theta)^2} \mid R_n \mid^2 e^{-\frac{d}{h_{int}}\xi(\Theta,\Phi)} \tag{1}$$

$$\xi(\Theta,\Phi) = \sqrt{1 + (\beta\gamma \sin\Theta \cos\Phi)^2} \tag{2}$$

where α is the fine-structure constant, N_W the number of grating periods, β=v/c the reduced electron velocity, Θ, Φ are the emission angles as introduced in Fig. 1. The interaction length

$$h_{int} = \frac{\beta\gamma}{4\pi}\lambda, \tag{3}$$

where $\gamma = (1-\beta^2)^{-1/2}$ is the Lorentz factor, describes the characteristic finite range of the virtual photons emitted and reabsorbed by the electrons and

$$\lambda = \frac{D}{\mid n \mid}(1/\beta - \cos\Theta), \tag{4}$$

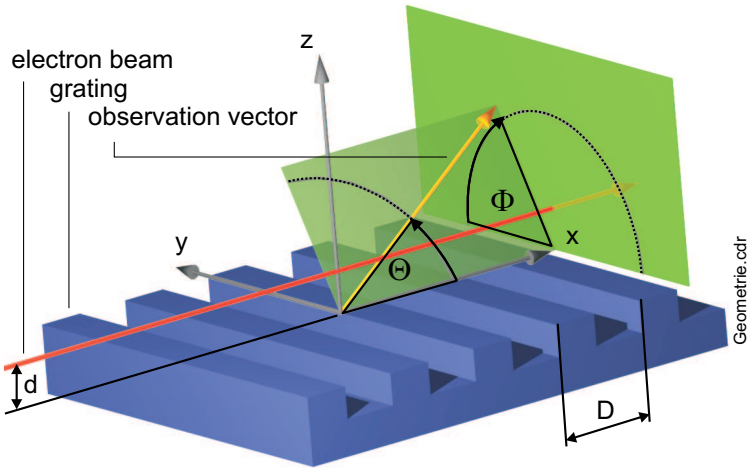

Figure 1. Definition of geometry. The electron moves with constant reduced velocity β=v/c at a distance d above the grating surface in x direction. The groves, oriented in the y direction, repeat with the grating period D. The photon wave-vector **k** makes the polar angle Θ with the positive x axis and the azimuthal angle Φ with the positive y axis in the plane spanned by the y and x axis

the wavelength of the emitted radiation. The quantity D is the grating period.

According to Eq. (1) the intensity decreases exponentially with increasing distance d between electron and grating surface. As shown by Fig. 2 (a), the normalized radial emittance ε_N^r of the electron beam restricts the minimum distance of the beam axis to the value

$$d_{min} = \sqrt{L\frac{\varepsilon_N^r/\pi}{\beta\gamma}}. \tag{5}$$

As has been discussed in detail in Ref. [Kube et al., 2002] the exponential coupling factor in Eq. (1) imposes restrictions on the wavelength and the grating length, see also Fig. 2 (a). These are relaxed to a great extent if the electron beam is guided in a strong magnetic field B, see Fig. 2 (b). The radius $R = 2\rho + r$ of an electron beam in the magnetic field can be described by the sum of the cyclotron radius $\rho = (p/(eB)) \cdot \vartheta$ and the radius r of the electron beam. The latter is connected to the transverse beam emittances ε_y and ε_z by the relation $\sqrt{\varepsilon_y\varepsilon_z/2} = \varepsilon_r = \pi \cdot \vartheta \cdot r$. A minimization with respect to the angle ϑ yields

$$\vartheta_{opt} = \sqrt{\frac{eB}{2m_e c}\frac{\varepsilon_N^r/\pi}{(\beta\gamma)^2}} \tag{6}$$

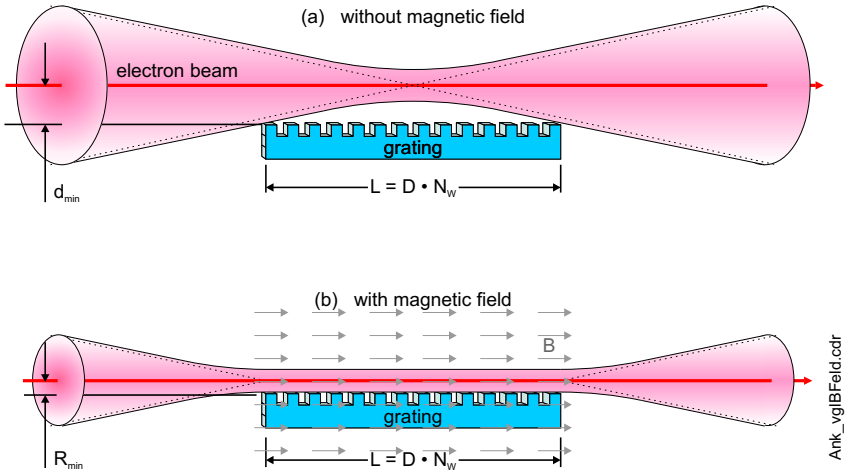

Figure 2. Coupling of an electron beam of finite emittance to the grating (a) without magnetic guiding field, and (b) with magnetic guiding field

and

$$R_{opt} = \sqrt{8\frac{m_e c}{eB}\frac{\varepsilon_N^r}{\pi}}. \tag{7}$$

With $h_{int} = \kappa \cdot R_{opt}$, and $\kappa \geq 1$ a coupling parameter, a critical wave length

$$\lambda_{crit} = \frac{8\sqrt{2}\pi\kappa}{\beta\gamma}\sqrt{\frac{m_e c}{eB}\frac{\varepsilon_N^r}{\pi}}. \tag{8}$$

can be defined which has no functional dependence on the length of the grating anymore. The meaning of this quantity is that for operational wavelengths $\lambda \leq \lambda_{crit}$ the radiation production mechanism becomes inefficient. In the above equations m_e is the rest mass of the electron.

The intensity $dN/d\Omega$ of the emitted radiation, Eq. (1), maximizes for Φ_{opt} = 90° and

$$\cos\Theta_{opt} = \beta = \sqrt{1 - 1/\gamma^2}. \tag{9}$$

Eqns. (4), (8), and (9) reduce to the optimum grating period

$$D_{opt} = \beta\gamma^2\lambda_{crit}. \tag{10}$$

Financial restrictions fixed the length of the grating and the magnetic field to L = 200 mm and B = 5 Tesla, respectively. With these parameters settled the

additional restriction that the grating should have at least $N_W \geq 100$ periods defines the region of operation, see Fig. 3.

As will be pointed out in the next subsection in more detail the Self Amplified Spontaneous Emission (SASE) amplification mechanism is driven by micro bunching of the electron beam. The relevant quantity to achieve micro bunching is the acceleration imposed on the electrons by the evanescent electric field. At constant force the acceleration scales as γ^{-3}. As a consequence, an electron beam energy as small as possible should be chosen. However, Fig. 3 tells that the THz gap can be accessed only by electron beams with an energy greater than about 1 MeV provided the normalized radial emittance is small enough, $\varepsilon_N^r \leq 2 \cdot 10^{-7}\pi$ m rad. The lowest energy at which the MAMI injector can be operated in a stable mode was found to be 1.44 MeV. With a normalized emittance ε_N^r = 66 $\cdot$ $10^{-9}\pi$ m rad and κ = 2 we obtain Θ_{opt} = 15.18°, h_{int}= 29.3 μm, λ_{crit} = 91.5 μm, D_{opt} = 1.121 mm, and at ϑ_{opt}= 2.67 mrad a R_{opt}= 13.4 μm. For the sake of simplicity we have chosen as design parameters λ = 100 μm, Θ_{opt} = 15.18°, and a grating period D = 1.4068 mm.

Finally, the radiation factors $\mid R_n \mid^2$ in Eq. (1) remains to be discussed. First of all a suitable shape of the grating structure must be chosen. We decided to use a lamellar, i.e. a rectangular, shape because it can easily be manufactured. The relevant parameters of such a grating are the ratio h/D of the groove depth to the grating period D, and the ratio a/D of the lamella width, i.e. the remaining material between the grooves, both taken with respect to the grating period D. The optimization was performed numerically by a modal expansion of the integral representation of the field inside the grooves using a Green's function formalism as described by Van den Berg [Van den Berg, 1974]. The procedure yielded a/D = 0.505 and h/D = 0.086 with a mean radiation factor $\langle \mid R_1 \mid^2 \rangle_\Theta$ = 0.23 [Rochholz, 2002].

These considerations define the experimental parameters and the experimental setup to be described in the following section.

Coherent Enhancement and Self Amplified Spontaneous Emission

For our research program to investigate radiation production mechanisms in the wavelength region between 30-300 μm special emphasis was put on amplification processes, in particular the coherent enhancement of Smith-Purcell radiation by a bunched beam and the Self Amplified Spontaneous Emission (SASE).

The radiated number of photons $\langle dN/d\Omega \rangle_{coh}$ from a bunch of N_e electrons, distributed according to Gaussians with a standard deviations σ_x, σ_y, and σ_z in the longitudinal x and transverse y and z directions, enhances with respect to

Eq. (1) by a factor $N_e(S_{inc}+(N_e-1)S_{coh})$. The incoherent S_{inc} and coherent S_{coh} form factors are given by [Doria et al., 2002]

$$S_{inc} = \frac{1}{\sqrt{2\pi}\sigma_z}\int_0^\infty e^{-z\ \xi(\Theta,\Phi)/h_{int}} e^{-(z-d)^2/2\sigma_z^2} dz \tag{11}$$

$$\begin{aligned} S_{coh} &= \Big|\frac{1}{\sqrt{2\pi}\sigma_z}\int_0^\infty e^{-z\ \xi(\Theta,\Phi)/2h_{int}} e^{-(z-d)^2/2\sigma_z^2} dz\Big|^2 \\ &\times\Big|\frac{1}{\sqrt{2\pi}\sigma_x}\int_{-\infty}^\infty e^{-ik_x x} e^{-x^2/2\sigma_x^2} dx\Big|^2 \\ &\times\Big|\frac{1}{\sqrt{2\pi}\sigma_y}\int_{-\infty}^\infty e^{-ik_y y} e^{-y^2/2\sigma_y^2} dy\Big|^2. \end{aligned} \tag{12}$$

The integrals in the longitudinal x and transverse y directions have been evaluated for $k_x = k/\beta = \omega/(c\beta) = 2\pi/(\beta\lambda)$ and $k_y = 0$ yielding $S_{coh,x} = \exp(-(2\pi\sigma_x/(\beta\lambda))^2)$ and $S_{coh,y} = 1$, respectively. The quantity d denotes the center of gravity of the Gaussian in z direction.

SASE occurs if the electron beam bunch will additionally be micro-bunched while the passage over the grating. This process is driven by longitudinal forces originating from evanescent surface fields which travel synchronously with the electron bunch across the grating. Gain formulas were derived by Wachtel [Wachtel, 1979], Schächter and Ron [Schächter and Ron, 1989], as well as by Kim and Song [Kim and Song, 2001] in a two-dimensional model with continuous sheet currents. The gains according to Schächter and Ron, G_{SR}, and Kim and Song, G_{KS}, which were somehow modified by us to meet our experimental situation, are

$$G_{SR} = \frac{\sqrt{3}}{2(\beta\gamma)^2}\Big(\frac{\beta c\overline{I}}{f_b F_{duty}\sqrt{2\pi}\sigma_x}\frac{4\pi\beta}{I_A\sqrt{2\pi}\sigma_z}(\frac{2\pi}{\lambda})^2 e^{-d/h_{int}} F(\Delta_z)\Big)^{1/3} \tag{13}$$

$$G_{KS} = \frac{\sqrt{2\pi}}{(\beta\gamma)^2}\Big(\frac{\beta c\overline{I}}{f_b F_{duty}\sqrt{2\pi}\sigma_x}\frac{e_{00}}{I_A\sqrt{2\pi}\sigma_z}\cdot\frac{2\pi}{\lambda} e^{-d/h_{int}} F(\Delta_z)\Big)^{1/2}, \tag{14}$$

respectively. The weighting function

$$F(\Delta_z) = \frac{\sinh(\Delta_z/2h_{int})}{\Delta_z/2h_{int}} \tag{15}$$

takes into account that in our experiment the transverse beam profile is in good approximation a Gaussian with standard deviation σ_z while in Ref. [Schächter and Ron, 1989] and in Ref. [Kim and Song, 2001] a rectangular shape of the transverse beam profile with a width Δ_z and a thin current sheet along the grating surface were assumed, respectively. Both quantities are connected by $\Delta_z = \sqrt{2\pi}\sigma_z$. Further on, I_A = ec/r_e = 17045.09 A is the Alfvén current,

with r_e the classical electron radius, and e_{00} the reflection coefficient to the $n = 0$ mode of the grating [Kim and Song, 2001].

The emitted power d^2P per unit solid angle $d\Omega$ and unit path length dx at a mean beam current $\overline{I}$ of duty cycle F_{duty}, and bunch repetition rate f_b is given by

$$\begin{aligned}\frac{d^2P}{d\Omega\, dx} &= \frac{2\pi\hbar c}{\lambda}\cdot\frac{\overline{I}}{e}\cdot\frac{dN}{d\Omega}\cdot\frac{1}{L}\Big[e^{2G\cdot x}S_{inc}+(\frac{\overline{I}}{ef_bF_{duty}}-1)S_{coh}\Big] \\ &= 2\pi c m_e c^2\frac{\overline{I}}{I_A}n^2\frac{1}{D^2}\frac{\sin^2\Theta\sin^2\Phi}{(1/\beta-\cos\Theta)^3}\mid R_n\mid^2 \\ &\quad\times\Big[e^{2G\cdot x}S_{inc}+(\frac{\overline{I}}{ef_bF_{duty}}-1)S_{coh}\Big]. \qquad (16)\end{aligned}$$

The total emitted power dP per unit solid angle $d\Omega$ is obtained by integrating over the grating length coordinate x:

$$\begin{aligned}\frac{dP}{d\Omega} &= 2\pi c m_e c^2\frac{\overline{I}}{I_A}n^2\frac{L}{D^2}\frac{\sin^2\Theta\sin^2\Phi}{(1/\beta-\cos\Theta)^3}\mid R_n\mid^2 \\ &\quad\times\Big[\frac{e^{2G\cdot L}-1}{2G\cdot L}S_{inc}+(\frac{\overline{I}}{ef_bF_{duty}}-1)S_{coh}\Big]. \qquad (17)\end{aligned}$$

A few remarks seem to be appropriate concerning the validity of Eqns. (13), (14), (16), and (17). These equations only hold if the bunch is sufficiently long to allow a micro-bunching of the electron plasma in the synchronously travelling evanescent surface mode. Such plasma waves have recently been investigated theoretically by Andrews and Brau [Andrews and Brau, 2004] who also derived a gain formula. One important result is that the evanescent mode has a wavelength somewhat larger as the longest wavelength of SP radiation which in fact is emitted in backward direction. If the results, which were derived for a special SP experiment [Urata et al., 1998], could be generalized the gain of Ref. [Andrews and Brau, 2004] is lower than the formula of Schächter and Ron predicts but higher as that of Kim and Song. Further on, it must be concluded from this work that the bunch length should be at least of the order of the wavelength of the backward emitted SP radiation $D(1/\beta+1)$, see Eq. (4), otherwise the gain is expected to be lower as the gain formulas predict, i.e. for an already bunched beam the gain is a function of the bunch length itself, or the coherent bunch form factor S_{coh}. In the limiting case of an already coherently emitting bunch it is reasonably that the gain must be negligible small. Inspecting Eq. (17) we see that SASE can be neglected if $GL \ll 1$, i.e. for a grating of length $L = 0.2$ m, as in our experiment, for $G \ll 5/\mathrm{m}$.

Let us finally discuss the ansatz in the square brackets of Eq. (16). Since the gain formulas were derived for initially incoherently emitting electrons we assumed that the gain factor acts only on the incoherent part. This ansatz should

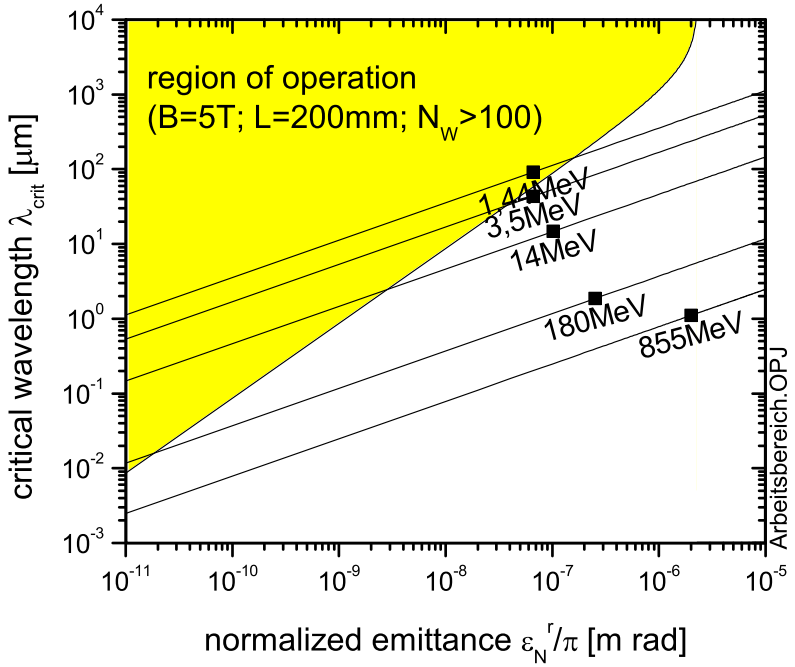

Figure 3. Critical wavelength λ_{crit} in first order $\mid n \mid = 1$ as function of the normalized radial emittance ε_N^r for different beam energies. The region of operation is indicated for a grating with length L = 200 mm, number of periods $N_W \geq 100$, and magnetic field B = 5 Tesla.

be a good approximation as long as the coherent form factor is small in comparison to the incoherent one, i.e. for $S_{coh} \ll S_{inc}$. For an already nearly coherently emitting bunch the gain formulas must be modified, as already mentioned above. However, our ansatz in the square brackets might still be right if such modified gain expressions would be used.

In Fig. 4 the gains of Ref. [Schächter and Ron, 1989; Kim and Song, 2001] are shown as function of the mean electrical beam current $\overline{I}$ for our experimental design parameters. The gain of Kim and Song is more than a factor 10 smaller than that of Schächter and Ron, and SASE for the former is expected to be negligible small. However, it must be stressed that in view of the discussion of the last paragraph the gain of Schächter and Ron constitutes most probably only an upper limit.

The emitted intensity as function of mean beam current $\overline{I}$ and distance d of the beam to the grating are shown in Fig. 5 and 6, respectively. The effect of coherent emission from the electron bunch does not exceed about 30 %. On the one hand, the large gain according to Schächter and Ron results for a constant

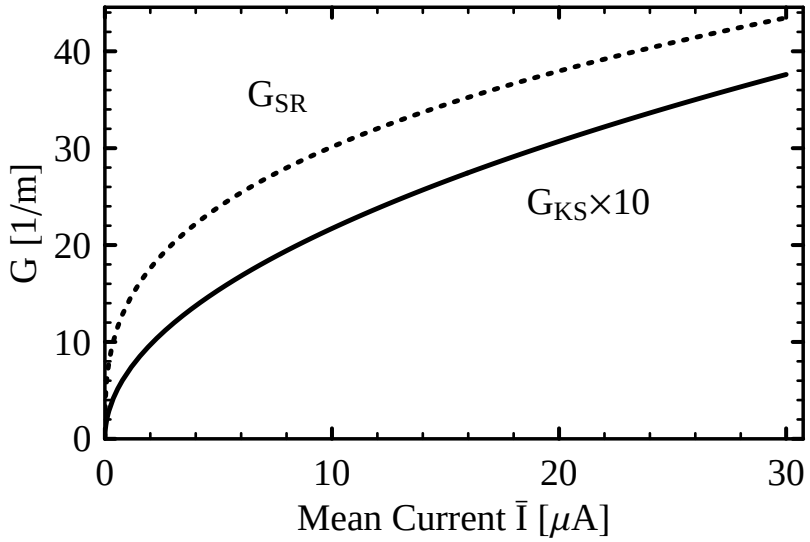

Figure 4. Gain G_{SR}, and G_{KS} according to Schächter and Ron [Schächter and Ron, 1989], and Kim and Song [Kim and Song, 2001], respectively, as function of the mean electron beam current $\overline{I}$. Parameters: kinetic energy of the electron beam 1.44 MeV, duty factor $F_{duty} = 0.5$, bunch repetition rate $f_b = 2.45$ GHz, standard deviation of bunch length σ_x = 256.9 μm, standard deviation of transverse beam size σ_z= 15 μm, radiation factor $\mid e_{00} \mid$ = 1, magnetic field B = 5 Tesla, distance of beam to the grating d = 30 μm, observation angle Θ = 15.2°, wave length λ = 100 μm

d in a strong nonlinear increase of the emitted intensity as function of $\overline{I}$. On the other hand, at constant $\overline{I}$ the intensity drops off faster as the interaction length h_{int} predicts for spontaneous emission. Both predictions can experimentally be scrutinized. It was one of the goals of the experiments described in the next subsection to shed light on this rather perturbing theoretical situation.

2. Experimental

Beam line and experimental setup at the 3.41 MeV injector of the Mainz Microtron MAMI for the investigation of the far-infrared Smith-Purcell radiation are shown in Fig. 7 and Fig. 8, respectively.

The 5 Tesla superconductive magnet (5T Cryomagnet System, manufactured by Cryogenic Ltd, UK London, Job J1879) has a bore of 100 mm diameter. The magnetic field of the solenoid was carefully mapped with a three dimensional Hall probe [Rochholz, 2002]. Along the grating with 200 mm length the magnetic field has a homogeneity of $|\Delta B|/B = 1.15 \cdot 10^{-3}$. More importantly, however, is the question for a bending of the magnetic field lines. Already a bending radius of R_0 = 390 m would be sufficient to prevent an optimal coupling of the electron beam with a radius of R = 15 μm to the grating.

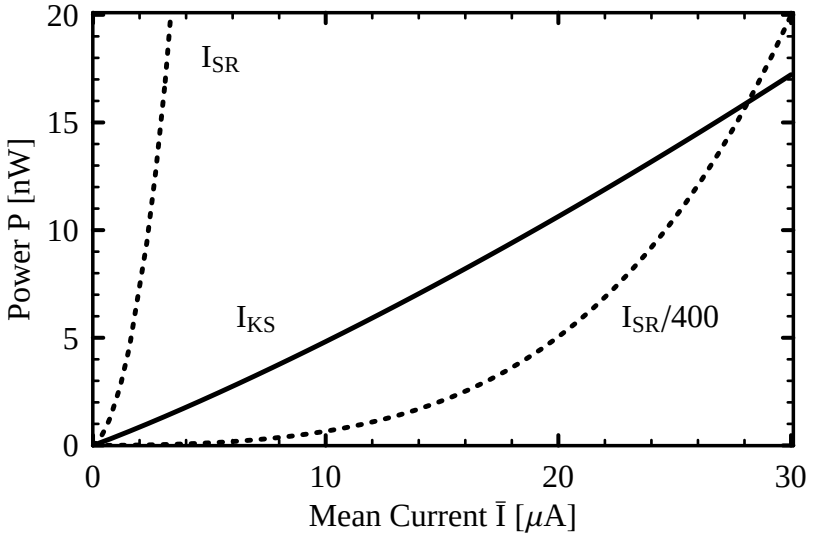

Figure 5. Integrated power in the limits $12.2^\circ \leq \Theta \leq 18.2^\circ$ and $60^\circ \leq \Phi \leq 120^\circ$ as function of the mean electron beam current $\overline{I}$. Shown are calculations with the gain of Kim and Song, labelled I_{KS}, and of Schächter and Ron, labelled I_{SR}. Radiation factor $|R_1|^2 = 0.23$, distance of the beam to the grating d = 30 μm, all other parameters as for Fig. 4

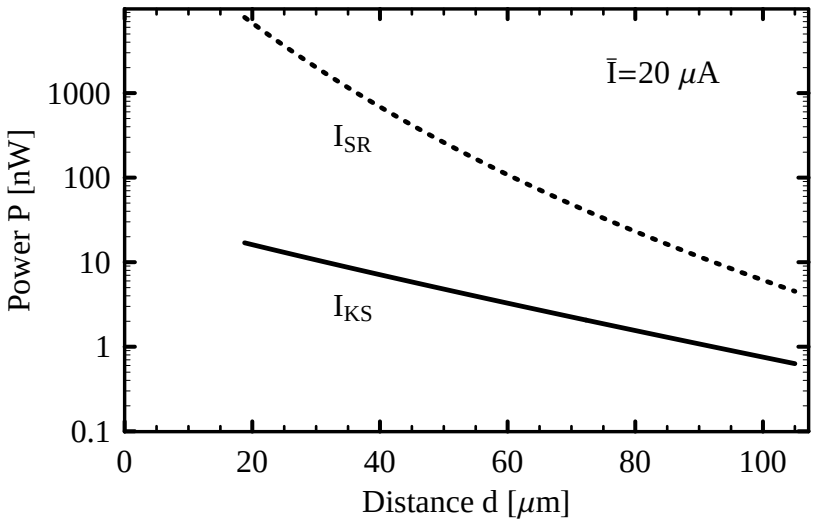

Figure 6. Integrated power in the limits $12.2^\circ \leq \Theta \leq 18.2^\circ$ and $60^\circ \leq \Phi \leq 120^\circ$ as function of the beam distance d from the grating. Shown are I_{KS} and I_{SR} according to the gain of Kim and Song and of Schächter and Ron, respectively. Radiation factor $|R_1|^2 = 0.23$, mean electron beam current $\overline{I}$ = 20 μA, all other parameters as quoted in Fig. 4

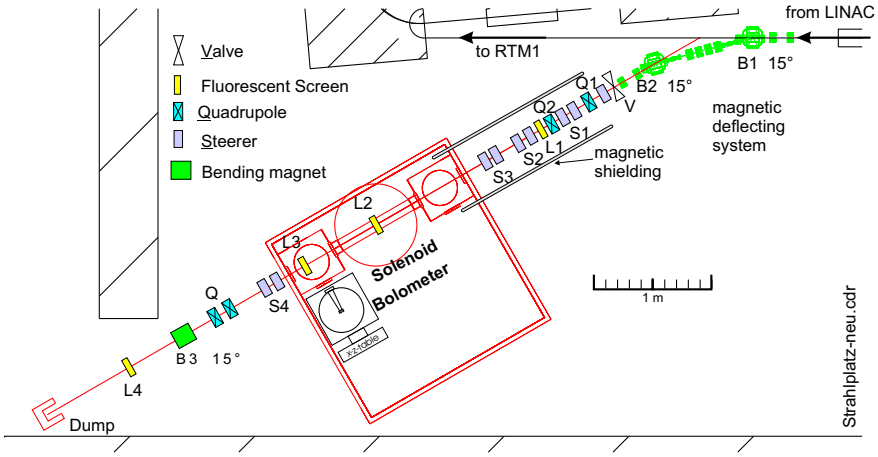

Figure 7. Setup of the Smith-Purcell experiment at the injector LINAC A of the Mainz Microtron MAMI. The 1.44 MeV electron beam is deflected just in front of the 14 MeV Race Track Microtron RTM1 by an angle of totally 30°. An achromatic and isochronous system has been employed, consisting of two bending magnets (B1, B2) and six quadrupoles. The beam is properly coupled into the superconductive solenoid by means of a quadrupole doublet (Q1, Q2) and steerer magnets (S1, S2, S3, S4). Stray fields are symmetrized in this region by a magnetic mu-metal shielding. Downstream the solenoid the beam is deflected downwards by an angle of 15° (bending magnet B3) and finally dumped. Three zinc sulfide fluorescent screens (L1, L2, L3, L4) serve for beam diagnostic purposes.

The relevant quantity is the inverse bending radius which in a two dimensional model is given by $1/R_0 = (\partial B/\partial z)/B_0$. Here z is the coordinate in the horizontal plane perpendicular to the symmetry axis. The measurement yielded $(\partial B/\partial z)/B_0 \leq 2.6{\cdot}10^{-5}$ cm^{-1} and fulfills the requirement within a region Δz = $\pm$ 1.4 mm.

The liquid helium cooled composite silicon bolometer (Mod. QSIB/3, manufactured by Composite Bolometer System, QMC Instruments Ltd, UK West Sussex) served as radiation detector. A low-pass and a high-pass filter restrict the sensitive spectral range to 33 μm $\leq \lambda \leq$ 2 mm. The f/3.5 Winston cone with an entrance aperture of 11 mm accepts angles $\theta \leq 8.1°$. The optical responsivity amounts to 10.7 kV/W , the speed of response is 285 Hz, and the system optical Noise Equivalent Power (NEP) 4.2 pW/$\sqrt{Hz}$ at 80 Hz. In combination with a lock-in amplifier the bolometer is sensitive enough to detect radiation under experimental conditions with a power as low as about 100 pW.

A special operating mode of the three linac sections was required to prepare a 1.44 MeV electron beam with good emittance and short bunch length

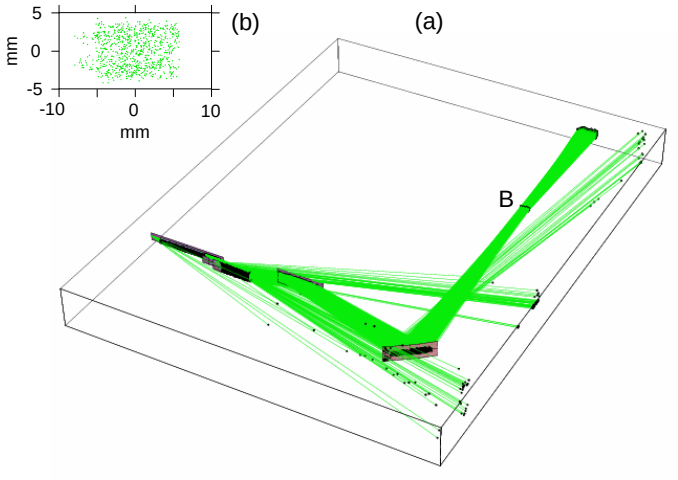

Figure 8. (a)View onto the optical system. Far-infrared radiation produced by the grating G of 200 mm length is vertically focused by a cylindrical mirror M1 deflected by a plane mirror M2 onto a horizontally focusing mirror M3 and detected by a bolometer B. A cylindrical mirror above the grating focuses the radiation back to the electron beam. All components are plated with a layer of 5 μm of gold. Shown are also ray trace simulations. (b) Ray distribution perpendicular to the nominal ray direction at the bolometer position B.

[Mannweiler, 2004]. The most critical part, however, was the injection of the beam into the solenoid since, first of all, the beam axis must exactly coincide with the symmetry axis of the magnetic field. To achieve this goal any field distortions, even as far away as 2 m from the entrance of the solenoid, must be avoided. The iron joke of the RTM1 was identified to be particularly sensitive to such field distortions and the entrance region of the solenoid had to be shielded over a length of 1.5 m by mu metal. In case the beam axis does not exactly coincide with the symmetry axis of the solenoidal magnetic field the beam spot describes a circle at the fluorescent screen behind the solenoid if the magnetic field is varied. The injection of the beam can this way be controlled and optimized. Secondly, the beam must be focussed in such a manner to accomplish in the solenoid the required optimal angle ϑ_{opt}, Eq. (6), which is correlated to the beam radius R_{opt}. For this purpose the beam spot size was measured in the solenoid by the secondary electron signal from a scanner wire of 40 μm thickness.

Finally, ray trace calculations were performed with the add-on Optica [Barnart, 2003] to Mathematica [Wolfram, 2003] to get insight into the focusing properties and efficiency of the optical system which guides the far-infrared radiation into the bolometer. The results are shown in figure 8. Initial coordinates and emission angles of 1000 rays were randomly and homogeneously

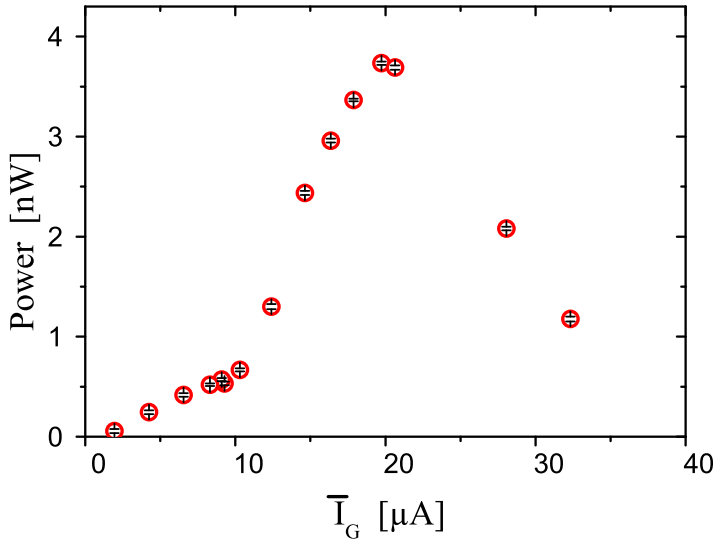

Figure 9. Bolometer signal as function of the mean beam current on the grating. Grating period 14.3 mm, wavelength λ = 1.0 mm at observation angle $\Theta = (15.2 \pm 3)^\circ$, accepted wavelength region of the bolometer 33 μm $\leq \lambda \leq$ 2 mm.

distributed on a 200 mm long line 10 μm above the grating in angular regions $12.2^\circ \leq \Theta \leq 18.2^\circ$ and $60^\circ \leq \Phi \leq 120^\circ$. Assuming that the grating has a reflectivity of 40 % for rays hitting the grating the efficiency of the optical system turns out to be 48 %. The bolometer was tuned into the spot shown in figure 8 (b) with the aid of a remote controlled two-dimensional parallel displacement support.

3. Results and Discussion

At the beam energy of 1.44 MeV we sought in a number of runs for spontaneous Smith-Purcell radiation with a wavelength of about 100 μm and, in particular, for the predicted SASE. Parameters and experimental setup were chosen as described above. Finally, only an upper limit $P \leq 0.085$ nW for the Smith-Purcell signal could be determined at a mean beam current $\bar{I}$ = 16 μA and a magnetic field B = 4.8 Tesla. The only reasonable explanation for this rather disappointing result is that the beam spot was larger than expected and, therefore, the beam could not be coupled optimally to the grating. One or a combination of the following reasons may be responsible: (i) the non-standard operation mode of the three MAMI Linac sections for the 1.44 MeV beam deteriorated the transverse emittance and, in addition, also the bunch length, (ii) the beam could not be injected into the solenoid in such a manner that the

optimal beam radius was achieved, and (iii) grating and electron beam in the solenoid could not be aligned properly. Indeed, measurements in the solenoid yielded a projected spot size in z direction with standard deviation of $\sigma_z \approx$ 100 μm. Also bunch length measurements were performed with the longitudinal phase space diagnostics of the injector linac [Euteneuer et al., 1988] which yielded σ_x = 540 μm. Assuming a distance d = 2.5 σ_z of the beam to the grating, even with the optimistic gain formula of Schächter and Ron an intensity of only P = 0.05 nW follows from the formulas presented in subsection 2 in accord with the experimental result.

To get further insight into the signal generation an experiment with a grating of the large period of 14.3 mm, a/D = 0.51, h/D = 0.09, $|R_1|^2$ = 0.24 was performed. The wavelength of the Smith-Purcell radiation at an emission angle of 15.2° amounts to λ = 1.0 mm. The interaction length h_{int} = 298 μm is large enough to couple even a beam with the experimentally determined large spot size of σ_z = 105 μm optimally to the grating. The intensity characteristics as function of the distance d of the electron beam from the grating was found to be consistent with the expected interaction length. The intensity of radiation as function of the grating current, see Fig. 9, was measured with half the electron beam current on the grating. The grating current, therefore, is the same as the current of the electrons above the grating which creates the Smith-Purcell radiation.

The non-linear growing of the signal as function of the current can be explained by the bunch coherence, as calculations with the above described formalism suggest, see figure 10 (a). The maximum of the intensity at a current of 20 μA and the decrease at larger currents is most probably a consequence of increasing bunch lengths, see figure 10 (b). It is worth mentioning that a gradual increase of the bunch length by only about 20 % explains already the experimentally observed dramatic decrease of the intensity at beam currents $I \geq$ 20 μA. These results are in accord with experiments to determine the shape of an electron bunch with the aid of coherent Smith-Purcell radiation, see e.g. Ref. [Doria et al., 2002], or [Korbly and A.S. Kesar, 2003].

The just described experiment with the 14.3 mm grating corroborate the conjecture that the required settings of the accelerator and beam line for an 1.44 MeV electron beam with low transverse spot size and short longitudinal bunch length in the solenoid were not found, or can not be achieved at all. Therefore, further experiments were performed with the 3.41 MeV standard beam of good quality the results of which will be reported elsewhere [Mannweiler, 2004].

4. Conclusions

Smith-Purcell (SP) radiation in the wave length region between 100 μm and 1000 μm has been investigated at the injector LINAC of the Mainz Microtron

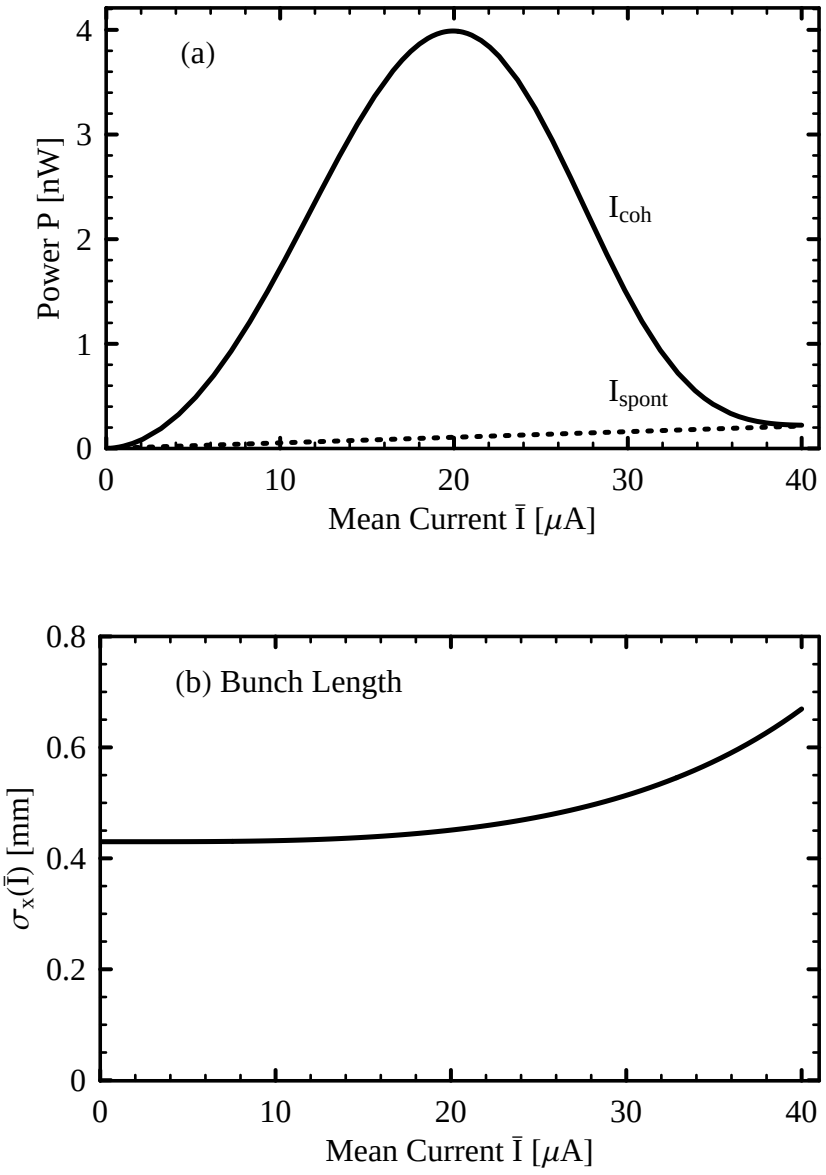

Figure 10. (a) Integrated intensity in the limits $12.2^\circ \leq \Theta \leq 18.2^\circ$ and $60^\circ \leq \Phi \leq 120^\circ$ as function of the mean electron beam current $\overline{I}$ for a grating with a period of 14.3 mm. Wave length λ = 1.0 mm at observation angle Θ = 15.2°. A rectangular beam profile of width Δ_z = 131.6 μm in z direction with a distance to the grating d = 65.8 μm was assumed. (b) Adapted standard deviation of the bunch length σ_x as function of the mean beam current $\overline{I}$. Other parameters: kinetic energy of the electron beam 1.44 MeV, duty factor $F_{duty} = 0.5$, bunch repetition rate $f_b = 2.45$ GHz, Δ_y = 263.2 μm, radiation factor $|R_1| = 0.23$, magnetic field $B = 4.8$ Tesla.

MAMI with a pulsed electron beam of 1.44 MeV energy. The beam was kept focused in a superconductive 5 Tesla magnet and guided above metal gratings with a length of 200 mm. The predicted large intensity of $\lambda = 100$ μm radiation at could not be observed. The most probable explanation for this fact is that (i) the beam spot size was too big and, therefore, the beam could not be coupled optimally to the grating, and (ii) gain formulas may not be applicable because the electron beam bunches in our experiment are shorter than the wavelength of the evanescent mode. At a wavelength of λ = 1 mm the observed intensity as function of the beam current can be explained by coherent emission from about 600 μm (rms) long electron bunches which slightly lengthen as the bunch charge increases.

Acknowledgments

One of us (H. M.) was supported during the course of this work by a stipend of the Studienstiftung des Deutschen Volkes. Part of this work has been supported by the Deutsche Forschungsgemeinschaft DFG under contract Ba1336/1-3.

References

Andrews, H. L. and Brau, C. A. (2004). *Phys. Rev. Spec. Topics - Acc. and Beams*, 7:070701.

Barnart, D. (2003) *Optica: Design Optics with Mathematica*. Wolfram Research. Version 1.3.0.

Di Francia, T. (1960). *Nuovo Cimento*, 16:61.

Doria, A., Gallerano, G., Giovenale, E., Messina, G., Doucas, G., Kimmitt, M. F., Andrews, H. L., and Brownell, J. (2002). *Nucl. Instr. Meth. in Phys. Res. A*, 483:263.

Euteneuer, H., Herminghaus, H., Nilles, K. W., and Schöler, H. (1988). In Tazzari, S., editor, *European Particle Accelerator Conference*, page 1149, Signapore, New Jersy, London, Hong Kong. World Scientific.

Frank, I. (1942). *Izv. Akad. Nauk SSSR, Ser Fiz.*, 6:3.

Kim, K. J. and Song, S. B. (2001). *Nucl. Instr. Meth. Phys. Res. A*, 475:158.

Korbly, S. E. and A.S. Kesar, M. A. Shapiro, R. J. T. (2003). In *Proceedings of the Particle Accelerator Conference*, page 2536.

Kube, G., Backe, H., Euteneuer, H., Grendel, A., Hagenbuck, F., Hartmann, H., Kaiser, K., Lauth, W., Schöpe, H., Wagner, G., Walcher, T., and Kretzschmar, M. (2002). *Phys. Rev. E*, 65:056501.

Mannweiler, H. (2004). Experimente zur Entwicklung eines Freie-Elektronen-Lasers auf der Basis des Smith-Purcell-Effektes im infraroten Spektralbereich, Dissertation, Institut für Kernphysik der Universität Mainz, 2004, in preparation.

Rochholz, H. (2002). Entwicklungsarbeiten für einen Freie-Elektronen-Laser auf der Basis des Smith-Purcell-Effektes im infraroten Spektralbereich, Diplomarbeit, Institut für Kernphysik der Universität Mainz, 2002, unpublished.

Schächter, L. and Ron, A. (1989). *Phys. Rev. A*, 40:876.

Smith, S. J. and Purcell, E. M. (1953). *Phys. Rev.*, 92:1069.

Urata, J., Goldstein, M., Kimmitt, M., Naumov, A., Platt, C., and Walsh, J. (1998). *Phys. Rev. Lett.*, 80:516.

Van den Berg, P. M. (1971). *Appl. Sci. Res.*, 24:261.
Van den Berg, P. M. (1973a). *J. Opt. Soc. Am*, 63:689.
Van den Berg, P. M. (1973b). *J. Opt. Soc. Am*, 64:1588.
Van den Berg, P. M. (1974). *J. Opt. Soc. Am*, 64:325.
Wachtel, J. M. (1979). *J. Appl. Phys.*, 50:49.
Wolfram, S. (2003). *Mathematica*. Wolfram Research. Version 5.0.